Biochemistry

Article

pubs.acs.org/biochemistry

A Rapid Analysis of Variations in Conformational Behavior during Dihydrofolate Reductase Catalysis

Robert L. Hughes, Luke A. Johnson, Enas M. Behiry, E. Joel Loveridge,[†] and Rudolf K. Allemann*

School of Chemistry, Cardiff University, Main Building, Park Place, Cardiff CF10 3AT, United Kingdom

Supporting Information

ABSTRACT: Protein flexibility is central to enzyme catalysis, yet it remains challenging both to predict conformational behavior on the basis of analysis of amino acid sequence and protein structure and to provide the necessary breadth of experimental support to any such predictions. Here a generic and rapid procedure for identifying conformational changes during dihydrofolate reductase (DHFR) catalysis is described. Using DHFR from *Escherichia coli* (EcDHFR), selective side-chain ^{13}C labeling of methionine and tryptophan residues is shown to be sufficient to detect the closed-to-occluded conformational transition that follows the chemical step in the catalytic cycle, with clear chemical shift perturbations found for both methionine methyl and tryptophan indole groups. In contrast, no such perturbations are seen for the DHFR from the psychrophile *Moritella profunda*, where the equivalent conformational change is absent. Like EcDHFR, *Salmonella enterica* DHFR shows experimental evidence of a large-scale conformational change following hydride transfer that relies on conservation of a key hydrogen bonding interaction between the M20 and GH loops, directly comparable to the closed-to-occluded conformational change observed in EcDHFR. For the hyperthermophile *Thermotoga maritima*, no chemical shift perturbations were observed, suggesting that no major conformational change occurs during the catalytic cycle. In spite of their conserved tertiary structures, DHFRs display variations in conformational sampling that occurs concurrently with catalysis.

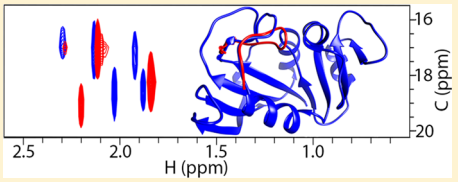

Protein motions play important roles in enzyme catalysis, and they are often necessary for progression through the catalytic cycle. Originally postulated more than half a century ago in Koshland's "induced fit" model,[1] conformational changes have only more recently been shown to be widely important for substrate binding and product release and to provide an optimal environment for catalysis.[2] Indeed, multiple enzyme families that display conserved motions during catalysis have been discovered, which indicates evolutionary pressures on both enzyme tertiary structures and the associated dynamics.[3,4] Members of the dihydrofolate reductase (DHFR) class of enzymes are considered to follow similar catalytic cycles and represent a classical enzyme model in which conformational changes occur within the catalytic cycle,[5] yet in different DHFR orthologs, variations in conformational dynamics have been identified.[6−11] Understanding this diversity of protein motions will in principle help to reveal their importance for the progression through the catalytic cycle and the influence of motions on catalytic proficiency.

DHFRs catalyze transfer of the *pro-R* hydride of reduced nicotinamide adenine dinucleotide phosphate (NADPH) to 7,8-dihydrofolate (DHF) to form 5,6,7,8-tetrahydrofolate (THF). THF acts as a one-carbon shuttle in the metabolism of purines, thymidylate, and certain amino acids and as a result is critical for cellular proliferation. As DHFR is paramount in maintaining the intracellular pool of THF, it has been a long-standing target for both antibacterial and antineoplastic drugs.[12] The canonical DHFR catalytic cycle, derived from studies of *Escherichia coli* DHFR (EcDHFR), exhibits five intermediate complexes[13] that adopt two distinct conformations, namely, closed and occluded (Figures 1 and 2).[7] EcDHFR contains three mobile loops within its structure: the highly mobile M20 loop (residues 9−24 by EcDHFR numbering), the FG loop (residues 116−132), and the GH loop (residues 142−149).[7] The holoenzyme (E:NADPH) first binds DHF to form the Michaelis complex (E:NADPH:DHF). In both these intermediates, a network of hydrogen bonds between residues in the M20 and FG loops stabilizes a closed conformation,[7] in which the enzyme possesses the optimal electrostatic environment for hydride transfer.[7,14] After product formation, these interactions are disrupted and new hydrogen bonds are established between the M20 and GH loops, stabilizing an occluded conformation, which is conserved in the three remaining intermediates (E:$NADP^+$:THF, E:THF, and E:THF:NADPH) of the catalytic cycle. Release of $NADP^+$ and rebinding of NADPH precede the release of THF from the active site, which at pH 7 is the rate-limiting step of the reaction.[7] Interchange between the closed and occluded conformations has been shown to modulate the affinity for the nicotinamide cofactor and to be important for product release.[7,13,15]

Variations in the conformational changes seen in EcDHFR have been identified in other DHFR homologues. For the DHFR from the psychrophile *Moritella profunda* (MpDHFR), which shares 55% sequence identity with EcDHFR,[16] the catalytic cycle progresses without the enzyme adopting the

Received: January 18, 2017
Revised: March 29, 2017
Published: April 3, 2017

DOI: 10.1021/acs.biochem.7b00045
Biochemistry 2017, 56, 2126−2133

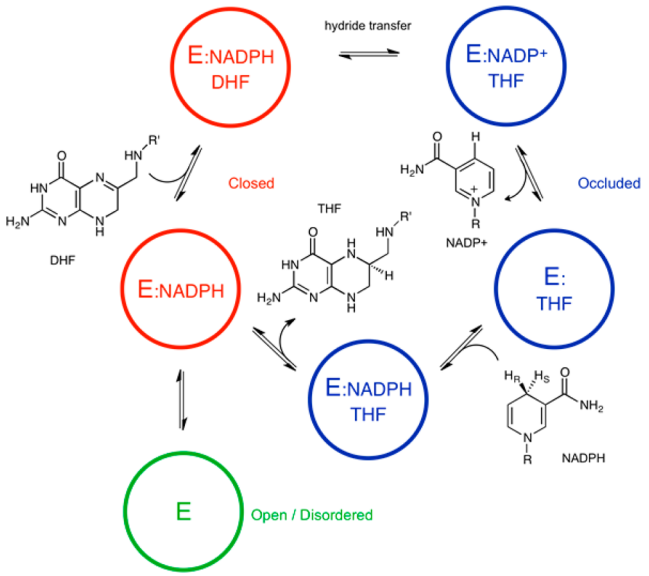

Figure 1. Catalytic cycle of EcDHFR under steady state conditions at pH 7. The major protein conformations adopted by the complexes in the catalytic cycle are indicated: open/disordered (green), closed (red), and occluded (blue).[7,23,24]

occluded conformation following hydride transfer,[10] even though the tertiary structures of EcDHFR and MpDHFR are nearly superimposable (Figure 2).[7,17] Crucially, hydrogen bonding between Ser148 and Asn23 is important for stabilizing the occluded conformation; it is abolished in MpDHFR because of a proline residue in place of Ser148.[10] Nonetheless, kinetically MpDHFR follows a catalytic cycle similar to that of EcDHFR, where release of product is the rate-limiting step under steady state conditions at pH 7.[17] The homodimeric DHFR from the hyperthermophile *Thermotoga maritima* (TmDHFR) exhibits a catalytic activity much lower than that of EcDHFR.[6,18,19] Residues corresponding to the FG loop in TmDHFR form part of the dimer interface, and TmDHFR is thought to proceed through the catalytic cycle in an open conformation, although fully conclusive experimental evidence is still lacking.[6,18,19]

Phylogenetic analysis indicates that among bacterial DHFRs there is diversity in whether the hydrogen bond donor and acceptor necessary to permit formation of the occluded conformation are present.[20] Meanwhile, for mammalian DHFRs, a proline rich region (PWPP) is inserted into the M20 loop, resulting in diminished flexibility.[11,21,22] This has been demonstrated to affect the stability of the occluded conformation, and the N23PP and N23PP/S148A variants of EcDHFR remain in the closed conformation after the chemical step and show reduced catalytic activity (diminished k_{cat}), with dissociation of $NADP^+$ becoming rate-limiting.[21] In contrast, EcDHFR-S148P cannot form an occluded conformation and displays an increased level of product inhibition, but the rate of hydride transfer is not significantly different from that of wild-type EcDHFR.[10] Together, these results indicate that while the occluded conformation has little influence on hydride transfer, it is important for modulating cofactor binding affinities and minimizing product inhibition.[10,21] Bacterial DHFRs that conserve the Asn23−Ser148 interaction or possess an equivalent stabilizing interaction should adopt conformations similar to that of the occluded conformation in EcDHFR.[10]

Although a wealth of kinetic and structural data is available for a number of DHFRs,[5] there currently exists no rapid and cost-effective method for assessing enzyme conformational states and loop dynamics for diverse DHFR orthologs. Notably, there are crystal structures of DHFRs from >20 organisms,[20] but these structures rarely describe the entire catalytic cycle and are often determined for apoenzymes or solely with the inhibitors methotrexate and trimethoprim. Moreover, for those DHFR structures that are anticipated to lack the occluded conformation, such as those for the enzymes from *Bacillius anthracis*[8] and *Lactobacillus casei*,[9,25] one can infer differences from only the model conformational cycle, because the absence of structural evidence of an occluded conformation does not necessarily imply that the conformation is not adopted. Here we demonstrate that by selective ^{13}C labeling of methionine and tryptophan side chains only, conformations in solution can be probed rapidly and highly cost-effectively by nuclear magnetic resonance (NMR) spectroscopy at different stages of the catalytic cycle for different DHFR orthologs. The reduced spectral complexity compared to those of more conventional backbone NMR methods aids interpretation and avoids more cumbersome assignment steps. We show that loop motions essential for progression through the catalytic cycle in EcDHFR are not necessary for efficient catalysis in other orthologs[7−9,13,25] and present the first clear experimental evidence in solution that TmDHFR remains in an open conformation throughout the catalytic cycle. Furthermore, we show that DHFR from *Salmonella enterica* (SeDHFR) exhibits conformational behavior similar to that of EcDHFR, in that it adopts an additional conformation after the chemical step. This work confirms the importance of hydrogen bonding interactions between the M20 and GH loops in stabilizing alternative occluded-like conformations within the product complex and demonstrates that EcDHFR is not unique in its ability to switch between conformations.

MATERIALS AND METHODS

Indole (2-^{13}C) was purchased from Cambridge Isotope Laboratories. $NADP^+$ and NADPH were purchased from Melford. DHF was produced by sodium dithionite reduction of folate as described previously.[26] All other chemicals, including L-methionine-(*methyl*-^{13}C), were from Sigma-Aldrich. DHFRs were grown in minimal medium and prepared as previously reported,[17] with the exception of the addition of either L-methionine-(*methyl*-^{13}C)[27] (80 mg L^{-1}) or indole-(2-^{13}C)[28] (50 mg L^{-1}) at an OD_{600} of 0.4. EcDHFR, MpDHFR, and SeDHFR were purified via anion exchange chromatography (Q-Sepharose) followed by size exclusion chromatography.[29] For SeDHFR, the procedure was adjusted from that published for EcDHFR and is outlined in Figure S1. TmDHFR was purified as previously described.[19] The SeDHFR encoding gene (Uniprot entry P12833) was purchased from Genscript within the pET-11b vector. The SeDHFR-S150A variant was prepared by standard site-directed mutagenesis methods with primers (Fwd, 5′ GCGGACGATAAGAACGCGTATGCGTGCGAG-TTTG 3′; Rev, 5′ CAAACTCGCACGCATACGCGTTCTT-ATCGTCCGC 3′) that were purchased from Sigma-Aldrich and expressed and purified as for wild-type SeDHFR.

All NMR experiments were performed on a Bruker AVANCE III 600 MHz (^1H) spectrometer equipped with a QCI-P cryoprobe and final enzyme concentrations of approximately 250 μM. EcDHFR, MpDHFR, and SeDHFR were prepared in 50 mM potassium phosphate buffer (pH 7.0)

DOI: 10.1021/acs.biochem.7b00045
Biochemistry 2017, 56, 2126−2133

containing 1 mM NaCl and 10 mM β-mercaptoethanol. TmDHFR was prepared in 50 mM Tris buffer (pH 7.0) containing 1 mM NaCl and 10 mM β-mercaptoethanol. Ligand stocks were pre-prepared at a concentration of 100 mM and pH 7, using extinction coefficients of 6200 cm^{-1} M^{-1} at 339 nm,[30] 17800 cm^{-1} M^{-1} at 260 nm,[31] and 28000 cm^{-1} M^{-1} at 282 nm[32] for NADPH, $NADP^+$, and folate/DHF, respectively. A 10-fold excess of ligands was used in each NMR experiment and the sample adjusted to pH 7.0 before measurement of the spectra, ensuring saturation (Table S1). To form the E:$NADP^+$:THF complex, NADPH and DHF were incubated with the enzyme for 20 min at 37 °C, with reaction completion and the absence of oxidation products confirmed by ^1H NMR. D_2O (10%) was added to all NMR samples. Spectra for MpDHFR, EcDHFR, SeDHFR, and TmDHFR were recorded at 7, 25, 25, and 40 °C, respectively, to maintain sample integrity and to be close to physiological conditions for each enzyme. Spectra were processed with NMRPipe[33] and analyzed using CcpNmr Analysis 2.4.1.[34]

With the exception of Met94, all methionine methyl resonances of MpDHFR had been published previously.[35] The assignment of the Met94 resonances was confirmed, and tryptophan indole-δ_1 resonances were assigned by re-evaluation of the three-dimensional (3D) ^{13}C- and ^{15}N-edited NOESY spectra acquired previously.[35] Each tryptophan indole NH resonance showed an intense NOESY crosspeak to a unique indole-δ_1 ^1H resonance observed here, readily allowing assignment. For EcDHFR, methionine methyl resonances and tryptophan indole-δ_1 resonances for EcDHFR were similarly assigned using 3D ^{13}C-edited NOESY, CCH-TOCSY, and HCCH-TOCSY spectra acquired on a Varian INOVA 800 MHz (^1H) spectrometer equipped with a cryogenically cooled HCN probe, using the 3D ^{15}N-edited NOESY spectrum acquired previously,[36] and by reference to published data.[37] The equation $\Delta\delta = [^1/_2(\delta_H^2 + \delta_C^2/4)]^{1/2}$ was used to obtain weighted average chemical shift perturbations.[38]

RESULTS AND DISCUSSION

To investigate the distribution of protein conformations during the catalytic cycle of different DHFR orthologs, EcDHFR and MpDHFR were first probed as models to identify whether systematical labeling of the proteins with [*methyl*-^{13}C]-methionine[27] and [indole-δ_1-^{13}C]tryptophan[28] could identify catalytic cycles that include or omit the occluded conformation. TmDHFR and SeDHFR were investigated to elucidate their conformational behavior, which had not been explored previously. Methionine comprises 3.1% of amino acid residues in MpDHFR and EcDHFR, 2.4% in TmDHFR, and 1.8% in SeDHFR, while tryptophan makes up 3.1% of the tryptophan amino acid residues in EcDHFR, 1.9% in MpDHFR and SeDHFR, and 0.6% in TmDHFR. This density ensured that a good description of protein conformational space was achieved without significant spectral crowding (Figure 2 and Figure S2).[6,7,17,18] In addition, a number of methionine and tryptophan residues are conserved in structurally significant positions.[6,7,16] Most notably, Trp22 in the M20 loop (Figure S2) is found in a wide range of DHFR orthologs and has been shown to be important for EcDHFR catalysis.[39] Similarly, Met42 is strongly conserved. In total, four of the five methionine residues in EcDHFR are conserved in MpDHFR (Met1, Met20, Met42, and Met92), and three of the five are conserved in SeDHFR (Met1, Met42, and Met92), although only Met44 is conserved in TmDHFR (Figure S2). The two

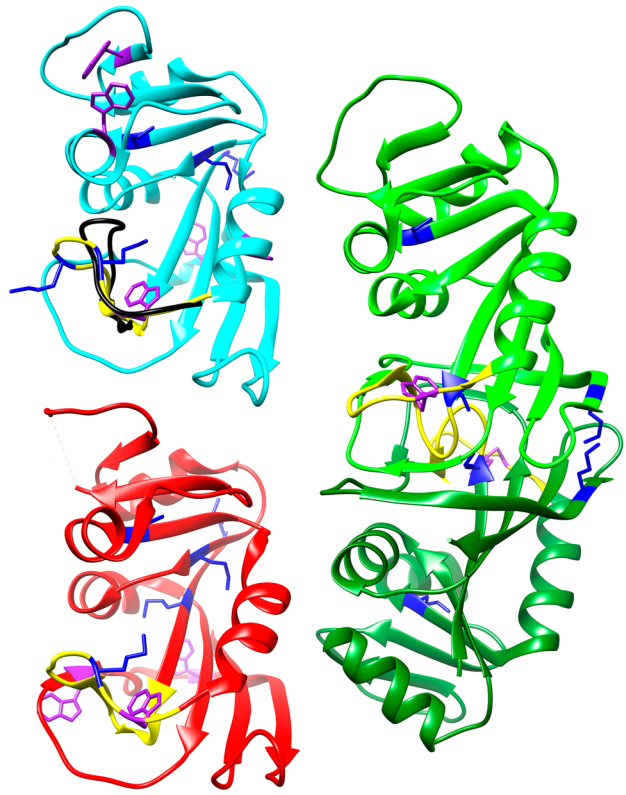

Figure 2. Cartoon representations of EcDHFR (cyan, PDB entry 1RX2[7]), TmDHFR (green, PDB entry 1D1G[6]), and MpDHFR (red, PDB entry 3IA5[29]). The "M20" loop in the occluded (black) and closed (yellow) conformations is highlighted as well as positions of methionine (blue) and tryptophan (purple).

remaining methionines in TmDHFR are located within the dimer interface. In addition to Trp22, EcDHFR, MpDHFR, and SeDHFR possess a Trp133 equivalent, although other tryptophan residues are well-dispersed throughout the protein structure. Met1 in TmDHFR is mostly removed during expression by an aminopeptidase present in *E. coli* (Figure S3).[40]

$^1H-^{13}C$ HSQC spectra of EcDHFR labeled with [*methyl*-^{13}C]methionine or [indole-δ_1-^{13}C]tryptophan (Figure 3A,B and Tables S2 and S3) exhibit five distinct cross-peaks corresponding to the five methionine and five tryptophan residues in the presence of ligands. The quality of the spectrum for [*methyl*-^{13}C]methionine-labeled apoenzyme was lower, with multiple minor cross-peaks observed for some residues (Figure S5). This is characteristic of spectra of apo-EcDHFR and apo-MpDHFR where the enzyme is in slow exchange between multiple conformational states.[36,41] Addition of ligands ($NADP^+$ and folate to model the Michaelis complex or $NADP^+$ and THF to form the product ternary complex) resulted in improved spectral quality, reduction in the number of cross-peaks, and increased resolution.[36] Complex formation also led to significant changes in chemical shift, indicative of the enzyme undergoing a transition to a new conformation. Dramatic changes in chemical shift were also observed between the E:$NADP^+$:folate and E:$NADP^+$:THF complexes, as the enzyme progressed to an occluded conformation after the chemical step. The largest chemical shift perturbations were exhibited by Met20 and Trp22, located in the highly flexible M20 loop; Met16, Met92, and Trp133 also showed notable changes.

DOI: 10.1021/acs.biochem.7b00045
Biochemistry 2017, 56, 2126−2133

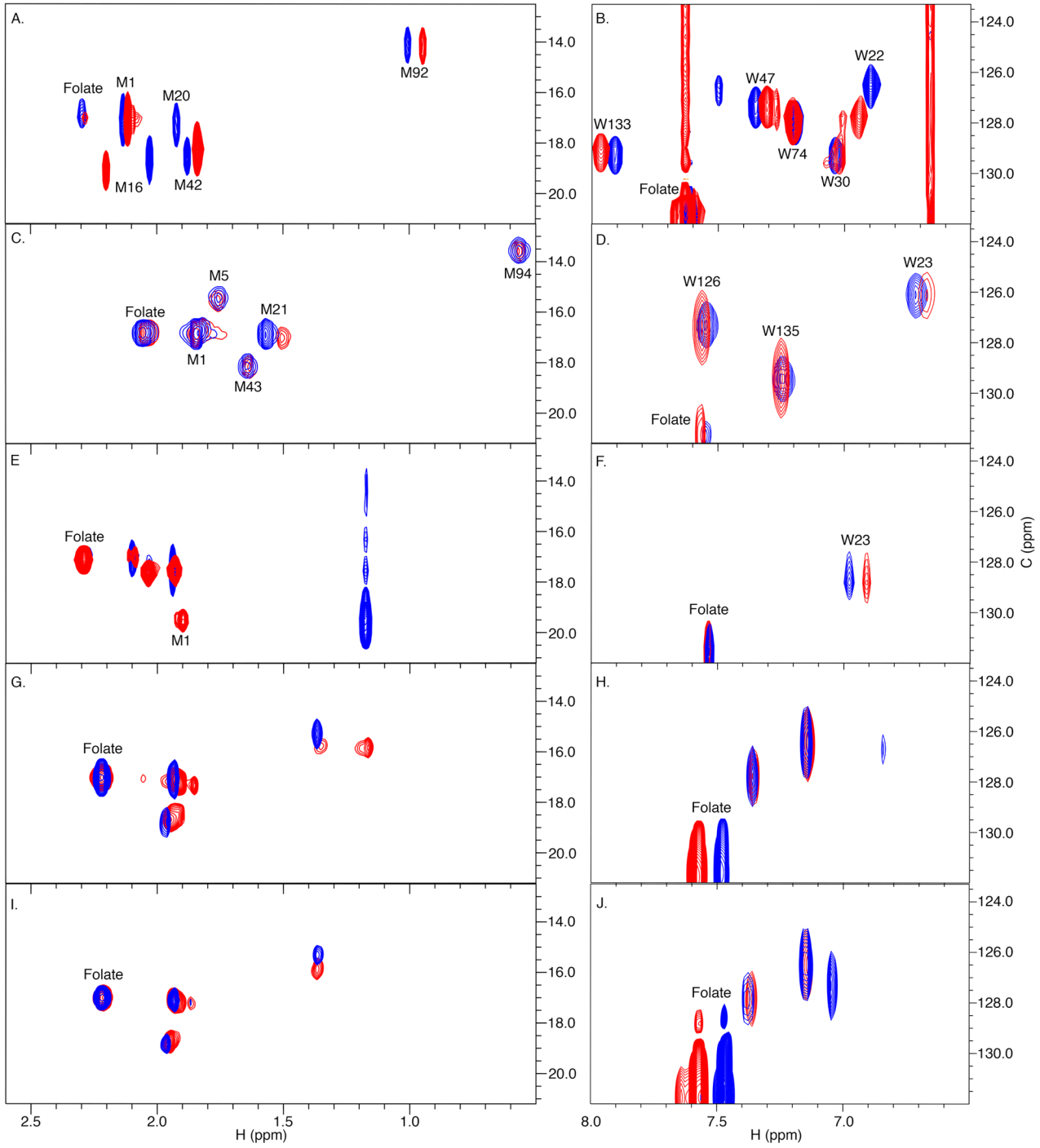

Figure 3. $^{1}H-^{13}C$ HSQC spectra of ^{13}C-labeled DHFR complexes, E:NADP^{+}:folate (closed conformation in EcDHFR) (blue) and E:NADP^{+}:THF (occluded conformation in EcDHFR) (red): (A) [*methyl*-^{13}C]methionine-labeled EcDHFR, (B) [δ_1-^{13}C]tryptophan-labeled EcDHFR, (C) [*methyl*-^{13}C]methionine-labeled MpDHFR, (D) [δ_1-^{13}C]tryptophan-labeled MpDHFR, (E) [*methyl*-^{13}C]methionine-labeled TmDHFR, (F) [δ_1-^{13}C]tryptophan-labeled TmDHFR, (G) [*methyl*-^{13}C]methionine-labeled SeDHFR, (H) [δ_1-^{13}C]tryptophan-labeled SeDHFR, (I) [*methyl*-^{13}C]-methionine-labeled SeDHFR-S150A, and (J) [δ_1-^{13}C]tryptophan-labeled SeDHFR-S150A.

As with the spectrum of [*methyl*-^{13}C]methionine-labeled apo-EcDHFR, the $^{1}H-^{13}C$ HSQC spectra of apo-MpDHFR labeled with [*methyl*-^{13}C]methionine or [indole-δ_1-^{13}C]tryptophan exhibited clear evidence of conformational heterogeneity (Figure S5). Again, addition of ligands led to an increase in spectral quality, indicative of the enzyme adopting one major conformation. $^{1}H-^{13}C$ HSQC spectra of the two complexes showed the expected five methionine and three tryptophan cross-peaks (Figure 3C,D). No significant change in chemical shift was observed between the Michaelis and product complexes for methionine or tryptophan residues (Tables S4 and S5). Notably, small changes in proton chemical shifts for Met21 and Trp23 were observed, but as these residues are directly adjacent to the site of chemistry, these most likely occur because of the differences in ligands, highlighting how it is important to differentiate between small changes that describe the changes at the site of chemistry and more

DOI: 10.1021/acs.biochem.7b00045
Biochemistry 2017, 56, 2126−2133

widespread chemical shift deviations, indicative of protein conformational changes as observed for EcDHFR.

The extensive differences in chemical shifts seen in the EcDHFR:$NADP^+$:folate and EcDHFR:$NADP^+$:THF complexes, as had previously been observed for [^{15}N]alanine-labeled EcDHFR,[42] provide clear evidence that methionine and tryptophan labeling is sufficient to observe the closed-to-occluded conformational change in EcDHFR. As expected, residues in the flexible M20 loop (Met16, Met20, and Trp22) all show large changes. Met16 in the apoenzyme and Michaelis complex appears to be solvent-exposed. However, in the product complex, the residue is located directly within the active site,[7] drastically changing the immediate molecular environment of the ^{13}C methyl group. Again, Met20 in the Michaelis complex points toward the FG loop, whereas in the product complex, it is more solvent-exposed, thus accounting for the observed downfield shift. Importantly, in EcDHFR, chemical shift changes are widely observed for all methionine and most tryptophan resonances, allowing binding effects of different ligands and deviations in protein conformation to be differentiated. No such widespread and significant changes in chemical shift were observed between the MpDHFR:$NADP^+$:folate and MpDHFR:$NADP^+$:THF complexes, confirming earlier work that suggested that MpDHFR does not adopt an occluded conformation after hydride transfer.[10] The results gained from EcDHFR and MpDHFR confirm that selective side-chain labeling can be used to identify whether an occluded-like conformation is adopted by a specific DHFR.

It has so far been challenging to investigate TmDHFR by conventional NMR methods because of poor tumbling in solution and fast T_2 relaxation as a consequence of its dimeric nature with a total molecular mass of 38k and its elongated shape.[18] Perdeuteration of TmDHFR to improve relaxation issues proved to be ineffective as the high thermal stability of TmDHFR prevented complete proton back-exchange of backbone amide groups in non-solvent-exposed regions (Figure S4). Consequently, three-dimensional NMR spectra of TmDHFR are of limited quality, and no triple-resonance assignment data for TmDHFR have been published. However, TmDHFR contains only three methionines and one tryptophan.[18] Because these side chains display superior relaxation properties, selective side-chain labeling can be used to explore the conformational dynamics of TmDHFR. ^{1}H−^{13}C HSQC spectra of TmDHFR exhibit four distinct methionine cross-peaks and one tryptophan cross-peak (Figure 3E,F). Met1 could be assigned as the intensity of this resonance was considerably lower than the others, as expected for a residue present in only ∼10% of the protein molecules because of aminopeptidase activity in *E. coli* (Figure S3). No significant changes in [*methyl*-^{13}C]methionine chemical shifts were observed between the apoenzyme and either complex (Tables S6 and S7). Trp23 displays a proton shift difference of 0.07 ppm between the Michaelis and product complexes, similar to that observed for MpDHFR. This difference is most likely due to different ligands, which are directly proximal to Trp23. These results suggest that TmDHFR adopts only a single major conformation in solution.

The occluded conformation has so far only been observed in EcDHFR, although some evidence of conformational flexibility following the chemical step has been reported for bacterial DHFRs.[11] We therefore tested our proposal that DHFR homologues that can form a hydrogen bond similar to the crucial Ser148−Asn23 interaction in EcDHFR will adopt a conformation similar to the occluded conformation found in EcDHFR. SeDHFR contains residues His24 and Ser150 in the equivalent positions (Figure S2), and the replacement of asparagine by histidine is not likely to have a negative effect because the hydrogen bonds are formed to the backbone amide and carbonyl of Asn23. SeDHFR should therefore adopt an occluded-like conformation following the chemical step. No NMR assignments or structural information currently exists for SeDHFR, although tentative assignment of methionine residues could be performed via sequence analysis, indicating that conserved residues are likely to reside in electronic environments similar to those in EcDHFR and MpDHFR. Like EcDHFR and MpDHFR, the quality of *methyl*-^{13}C spectra of the methionine-labeled SeDHFR apoenzyme was low as a consequence of conformational heterogeneity (Figure S5). SeDHFR exhibits three well-defined cross-peaks when in the E:$NADP^+$:folate complex. However, unlike EcDHFR, SeDHFR shows two distinct species in the E:$NADP^+$:THF complex; both species seem to be equally populated (Figure 3G,H). Half of the cross-peaks present in the product complex overlap with those present in the Michaelis complex, indicating that in the product complex SeDHFR is characterized by an equilibrium between the Michaelis conformation and a second conformational state (Tables S8 and S9). It is worth noting that changing Ser148 in EcDHFR leads to a destabilization of the occluded conformation.[21] To confirm whether the two observed species in SeDHFR related to similar conformational behavior, SeDHFR-S150A was prepared. In the product complex, two species were present in this variant, but the relative population of the two states was drastically shifted to favor the Michaelis complex (Figure 3I,J and Tables S10 and S11). This reinforced the idea that the chemical shift perturbations observed in Met94 and Met42 are likely to be caused by a conformational change resembling that found in EcDHFR and again confirmed the significance of the hydrogen bond interaction between the M20 and GH loops in its formation. No significant chemical shift perturbations were observed in the [indole-δ_1-^{13}C]-tryptophan-labeled SeDHFR, which in this instance proved not to be diagnostic of conformational change.

SeDHFR, unlike EcDHFR and MpDHFR, lacks methionine residues within the M20 loop, which directly participates in the closed-to-occluded conformational change. To provide further evidence that the second conformation present in the product complex of SeDHFR resembles the occluded conformation observed for EcDHFR, ^{1}H−^{15}N HSQC spectra of both the Michaelis and product complexes were recorded (Figures S6 and S7). As observed through the [*methyl*-^{13}C]methionine resonances, widespread chemical shift differences are found between the complexes, again justifying that simple side-chain labeling is sufficient to identify conformational change within DHFRs, even when the probes are not located directly within the site of conformational change. This suggested that SeDHFR does indeed form an occluded-like conformation.

In general, we found [*methyl*-^{13}C]methionine chemical shifts more diagnostic of DHFR conformational changes than those of [indole-δ_1-^{13}C]tryptophan. In all four DHFRs, Trp22 forms a hydrogen bond to bound folates. It would therefore be expected to show a difference in chemical shift between the apoenzyme and the two complexes. In MpDHFR and TmDHFR, Trp23 does indeed display small proton chemical shifts for each separate complex, while in contrast, no significant differences are observed for SeDHFR. A large

DOI: 10.1021/acs.biochem.7b00045
Biochemistry 2017, 56, 2126−2133

deviation is found for the Michaelis complex of EcDHFR, but apoenzyme and product complexes are similar. Taken together, this illustrates how ligand binding effects dominate for this residue because of its location adjacent to the site of chemistry, obscuring any chemical shift perturbations in response to protein conformational changes. Similarly, for the spectra of apo-EcDHFR, MpDHFR, and SeDHFR, the tryptophan data show no evidence of the conformational heterogeneity obviously present upon observation of [*methyl*-^{13}C]methionine spectra and previously reported.[28,43] Conformational changes can nonetheless be followed through [indole-δ_1-^{13}C]tryptophan labeling, because there is clear evidence for the closed-to-occluded transition in EcDHFR, which may simply be more evident for EcDHFR than for SeDHFR because of the larger number of [indole-δ_1-^{13}C]tryptophans present within its sequence.

Importantly, by combination of the [indole-δ_1-^{13}C]-tryptophan labeling with [*methyl*-^{13}C]methionine labeling, which could in principle have been performed in a single protein, clear evidence of large-scale protein conformational changes was found for EcDHFR and SeDHFR. In EcDHFR, the ability to switch to an occluded conformation is essential for progression through the catalytic cycle, but this had not previously been observed in other DHFRs.[10,11] Ser148 in EcDHFR, which forms two hydrogen bonds to the M20 loop, is replaced with proline in MpDHFR.[10] Consequently, M20 loop motions appear not to play a significant role in MpDHFR catalysis, and it was known that MpDHFR remains in a closed conformation throughout the catalytic cycle.[10,44] Switching from the closed to the occluded conformation immediately follows hydride transfer in EcDHFR, before release of $NADP^+$ from the product ternary complex.[45] Switching to the occluded conformation in EcDHFR lowers the binding affinity of $NADP^+$, mitigates possible product inhibition effects, and allows efficient progress through the catalytic cycle.[10,46] However, similar single-turnover rate constants for EcDHFR- and MpDHFR-catalyzed hydride transfer at pH 7 show that the ability to form the occluded conformation does not have a major effect on the chemical step. Hydride transfer in the occluded conformation is not possible because of the distance between the reactants.[10,36]

Despite the lack of assignment data for both Tm- and SeDHFR, important conclusions can be drawn from the data presented here. Side-chain labeling of methionine and tryptophan yields simple and intuitively useful data. Previous reports that TmDHFR remains in a fixed open conformation during catalysis were based upon two X-ray single-crystal structures, and neither of them effectively modeled the Michaelis or product complex.[18] Hence, here the first direct evidence that TmDHFR remains fixed in an open conformation throughout the catalytic cycle is reported. Any further emphasis is however limited for TmDHFR because of the different distribution of methionine residues to Ec- and MpDHFR and highlights how the distribution and conservation of labels can be potentially limiting when establishing conformational changes and comparing orthologs.

The ease of labeling meant that the conformational behavior of SeDHFR, for which no structural data exist, could be analyzed rapidly, and predictions based upon primary sequence analysis were verified. SeDHFR exists in multiple solution forms, and their assignment could be based on similarity to other DHFRs. Like EcDHFR, SeDHFR showed two conformations in the product complex, but the relative stability of two conformations was evidently different. The occluded conformation dominates in the product complex of EcDHFR, while in SeDHFR, the Michaelis conformation is still present at an approximately equimolar concentration. This difference may influence the kinetics of product release.

Principally selective side-chain ^{13}C labeling provides a rapid and cost-effective approach for surveying protein conformations during catalysis for multiple proteins, allowing more traditional and detailed analysis to be adjudged worthwhile. The cost of production of proteins labeled with [*methyl*-^{13}C]methionine (£11 per liter of culture) and [indole-δ_1-^{13}C]tryptophan (£96 per liter of culture) is considerably lower than that of triply (^{2}H, ^{13}C, ^{15}N, £622 per liter of culture) or doubly (^{13}C, ^{15}N, £262 per liter of culture) labeled proteins required for full NMR assignments (when accounting for 4 g L^{-1} [U-^{2}H,^{13}C]- or [U-^{1}H,^{13}C]glucose, respectively). Selective labeling also provides greatly simplified spectra, exhibiting only a fraction of the number of cross-peaks seen for fully labeled proteins, and the data can be acquired over much narrower spectral windows (10−14 ppm in ^{13}C rather than ∼70 ppm for a full aliphatic ^{1}H−^{13}C HSQC spectrum). In addition, $^{13}CH_3$ groups (as in [*methyl*-^{13}C]methionine) typically show high sensitivity in NMR experiments, because of the three equivalent protons,[43] and aliphatic ^{13}C shifts are most sensitive to conformational changes.[38] For DHFR, selective side-chain ^{13}C labeling is clearly sufficient to gain insight into large-scale protein motions that are important for progression through the catalytic cycle and expands upon previous work that demonstrated for EcDHFR the effectiveness of side-chain labeling methods in measuring picosecond to nanosecond time-scale protein dynamics.[47]

In conclusion, we have demonstrated here the utility of selective side-chain labeling to rapidly probe conformational behavior during DHFR catalysis. EcDHFR is known to undergo large-scale conformational changes along the catalytic cycle and shows clear chemical shift perturbations of its methionine methyl and tryptophan indole groups following the chemical step. MpDHFR, on the other hand, an enzyme known to maintain a single major conformation during catalysis, does not display such perturbations. Thermostable, homodimeric TmDHFR does not show any significant chemical shift perturbations following the chemical step, corroborating crystallographic evidence and providing the first direct evidence that this enzyme also adopts a single major conformation in solution. Conformational sampling is, however, not unique to EcDHFR, and DHFR from *S. enterica* exhibits similar conformational behavior, most likely adopting an occluded-like conformation. Clearly, amino acid sequence analysis allows the prediction of large-scale protein conformational behavior in DHFRs, and spectra obtained with site selectively labeled proteins may be readily interpreted even in the absence of resonance assignments. However, the scope of selective side-chain ^{13}C labeling is not limited to an analysis of structural events during DHFR catalysis and can be used to track conformational changes in a wide range of proteins.

■ ASSOCIATED CONTENT

Supporting Information

The Supporting Information is available free of charge on the ACS Publications website at DOI: 10.1021/acs.biochem.7b00045.

DOI: 10.1021/acs.biochem.7b00045
Biochemistry 2017, 56, 2126−2133

Purification procedure for SeDHFR and SDS-PAGE gel; amino acid sequence analysis of multiple DHFRs; mass spectrum of TmDHFR highlighting the presence of Met1; a modified version of Figure 3 including spectra for APO complexes; $^{1}H-^{15}N$ HSQC spectra of SeDHFR in both the Michaelis and product complexes and tables cataloguing the observed weighed chemical shift changes (PDF)

AUTHOR INFORMATION

Corresponding Author

*School of Chemistry, Cardiff University, Main Building, Park Place, Cardiff CF10 3AT, U.K. E-mail: allemannrk@cardiff.ac.uk. Phone: (44) 29 2087 9014.

ORCID

E. Joel Loveridge: 0000-0002-8528-4019

Rudolf K. Allemann: 0000-0002-1323-8830

Present Address

†E.J.L.: Department of Chemistry, Swansea University, Singleton Park, Swansea SA2 8PP, U.K.

Author Contributions

R.L.H. performed the experimental work. R.L.H., L.A.J., E.M.B., E.J.L., and R.K.A. designed the experiments and composed the manuscript.

Funding

This work was supported by the U.K. Biotechnology and Biological Sciences Research Council (BBSRC) through Grants BB/J005266/1, BB/L020394/1, and BB/M006158/1, by the Life Sciences Research Network Wales (an initiative funded through the Welsh Government's Sêr Cymru program), and by Cardiff University.

Notes

The authors declare no competing financial interest.

ACKNOWLEDGMENTS

We thank Dr. Sara Whittaker of the Biomolecular NMR Facility at the University of Birmingham for assistance with the operation of the Varian INOVA 800 MHz (^{1}H) spectrometer. The help of Dr. Rob Jenkins and Mr. Thomas Williams with mass spectrometry and NMR spectroscopy is gratefully acknowledged.

ABBREVIATIONS

DHFR, dihydrofolate reductase; EcDHFR, DHFR from *E. coli*; MpDHFR, DHFR from *M. profunda*; TmDHFR, DHFR from *T. maritima*; SeDHFR, DHFR from *S. enterica*; $NADP^{+}$, nicotinamide adenine dinucleotide phosphate; NADPH, nicotinamide adenine dinucleotide phosphate (reduced form); DHF, dihydrofolate; THF, tetrahydrofolate; PDB, Protein Data Bank.

REFERENCES

(1) Koshland, D. E. (1958) Application of a theory of enzyme specificity to protein synthesis. *Proc. Natl. Acad. Sci. U. S. A. 44*, 98–104.

(2) Karplus, M., and McCammon (1983) Dynamics of Proteins: Elements and Function. *Annu. Rev. Biochem. 52*, 263–300.

(3) Sawaya, M. R., and Kraut, J. (1997) Loop and subdomain movements in the mechanism of *Escherichia coli* dihydrofolate reductase: Crystallographic evidence. *Biochemistry 36*, 586–603.

(4) Katebi, A. R., and Jernigan, R. L. (2014) The critical role of the loops of triosephosphate isomerase for its oligomerization, dynamics, and functionality. *Protein Sci. 23*, 213–218.

(5) Luk, L. Y. P., Loveridge, E. J., and Allemann, R. K. (2015) Protein motions and dynamic effects in enzyme catalysis. *Phys. Chem. Chem. Phys. 17*, 30817–30827.

(6) Dams, T., Auerbach, G., Bader, G., Jacob, U., Ploom, T., Huber, R., and Jaenicke (2000) The crystal structure of dihydrofolate reductase from Thermotoga maritima: molecular features of thermostability. R. *J. Mol. Biol. 297*, 659–672.

(7) Sawaya, M. R., and Kraut, J. (1997) Loop and subdomain movements in the mechanism of *Escherichia coli* dihydrofolate reductase: Crystallographic evidence. *Biochemistry 36*, 586–603.

(8) Beierlein, J. M., Frey, K. M., Bolstad, D. B., Pelphrey, P. M., Joska, T. M., Smith, A. E., Priestley, N. D., Wright, D. L., and Anderson, A. C. (2008) Synthetic and Crystallographic Studies of a New Inhibitor Series Targeting *Bacillus anthracis* Dihydrofolate Reductase. *J. Med. Chem. 51*, 7532–7540.

(9) Feeney, J., Birdsall, B., Kovalevskaya, N. V., Smurnyy, Y. D., Navarro Peran, E. M., and Polshakov, V. I. (2011) NMR Structures of Apo *L. casei* Dihydrofolate Reductase and its Complexes with Trimethoprim and NADPH: Contributions to Positive Cooperative Binding from Ligand-Induced Refolding, Conformational Changes, and Interligand Hydrophobic Interactions. *Biochemistry 50*, 3609–3620.

(10) Behiry, E. M., Luk, L. Y. P., Matthews, S. M., Loveridge, E. J., and Allemann, R. K. (2014) Role of the occluded conformation in bacterial dihydrofolate reductases. *Biochemistry 53*, 4761–4768.

(11) Bhabha, G., Ekiert, D., Jennewein, M., Zmasek, C. M., Tuttle, L. M., Kroon, G., Dyson, J. H., Godzik, A., Wilson, I. A., and Wright, P. E. (2013) Divergent evolution of protein conformational dynamics in dihydrofolate reductase. *Nat. Struct. Mol. Biol. 20*, 1243–1249.

(12) Blakley, R. L. (1984) in *Folates and Pterins*, pp 191–253, Wiley, New York.

(13) Fierke, C. A., Johnson, K. A., and Benkovic, S. J. (1987) Construction and Evaluation of the Kinetic Scheme Associated with Dihydrofolate reductase from *Escherichia coli*. *Biochemistry 26*, 4085–4092.

(14) Loveridge, E. J., Behiry, E. M., Guo, J., and Allemann, R. K. (2012) Evidence that a 'Dynamic Knockout' in Escherichia coli Dihydrofate Reductase does not affect the chemical step of catalysis. *Nat. Chem. 4*, 292–297.

(15) McElheny, D., Schnell, J. R., Lansing, J. C., Dyson, H. J., and Wright, P. E. (2005) Defining the role of active-site loop fluctuations in dihydrolate reductase catalysis. *Proc. Natl. Acad. Sci. U. S. A. 102*, 5032–5037.

(16) Xu, Y., Feller, G., Gerday, C., and Glansdorff, N. (2003) *Moritella* Cold-Active Dihydrolate Reductase: Are There Natural Limits to Optimization of Catalytic Efficiency at low temperatures? *J. Bacteriol. 185*, 5519–5526.

(17) Evans, R. M., Behiry, E. M., Tey, L. H., Guo, J., Loveridge, E. J., and Allemann, R. K. (2010) Catalysis by dihydrofolate reductase from the psychropiezophile *Moritella* profunda. *ChemBioChem 11*, 2010–2017.

(18) Dams, T., Bohm, G., Auerbach, G., Bader, G., Schurig, H., and Jaenicke, R. (1998) Homo-dimeric recombinant dihydrofolate reductase from Thermotoga maritima shows extreme intrinsic stability. *Biol. Chem. 379*, 367–371.

(19) Maglia, G., Javed, M. H., and Allemann, R. K. (2003) Hydride Transfer During Catalysis by Dihydrofolate Reductase from *Thermotoga maritima*. *Biochem. J. 374*, 529–535.

(20) Hecht, D., Tran, J., and Fogel, G. B. (2011) Structural-based analysis of dihydrofolate reductase evolution. *Mol. Phylogenet. Evol. 61*, 212–230.

(21) Bhabha, G., Lee, J., Ekiert, D. C., Gam, J., Wilson, I. A., Dyson, H. J., Benkovic, S. J., and Wright, P. E. (2011) A dynamic knockout reveals that conformational fluctuations influence the chemical step of enzyme catalysis. *Science 332*, 234–238.

DOI: 10.1021/acs.biochem.7b00045
Biochemistry 2017, 56, 2126–2133

(22) Liu, C. T., Hanoian, P., French, J. B., Pringle, T. H., Hammes-Schiffer, S., and Benkovic, S. J. (2013) Functional significance of evolving protein sequence in dihydrofolate reductase from bacteria to humans. *Proc. Natl. Acad. Sci. U. S. A. 110*, 10159−10164.
(23) Falzone, C. J., Wright, P. E., and Benkovic, S. J. (1994) Dynamics of a flexible loop in dihydrofolate reductase from Escherichia coli and its impication for catalysis. *Biochemistry 33*, 439−442.
(24) Li, L., Falzone, C. J., Wright, P. E., and Benkovic, S. J. (1992) Functional Role of a Mobile Loop of *Escherichia coli* Dihydrofolate reductase in Transition State Stabilization. *Biochemistry 31*, 7826−7833.
(25) Gargaro, A. R., Soteriou, A., Frenkiel, T. A., Bauer, C. J., Birdsall, B., Polshakov, V. I., Barsukov, I. L., Roberts, G. C., and Feeney, J. (1998) The Solution Structure of the Complex of Lactobacillus Casei Dihydrofolate Reductase with Methotrexate. *J. Mol. Biol. 277*, 119−134.
(26) Blakley, R. L. (1960) Crystalline dihydropteroylglutamic acid. *Nature 188*, 231−232.
(27) Tzeng, S. R., Pai, M. T., and Kalodimos, C. G. (2012) NMR Studies of Large Protein Systems. *Methods Mol. Biol. 831*, 133−140.
(28) Rodriguez-Mias, R. A., and Pellecchia, M. (2003) Use of Selective Trp Side Chain Labeling To Characterize Protein-Protein and Protein-Ligand Interactions by NMR Spectroscopy. *J. Am. Chem. Soc. 125*, 2892−2893.
(29) Hay, S., Evans, R. M., Levy, C., Loveridge, E. J., Wang, X., Leys, D., Allemann, R. K., and Scrutton, N. S. (2009) Are the catalytic properties of enzymes from piezophillic organisms pressure adapted? *ChemBioChem 10*, 2348−2353.
(30) Allemann, R. K., Evans, R. M., Tey, L., Maglia, G., Pang, J., Rodriguez, R., Shrimpton, P. J., and Swanwick, R. S. (2006) Protein Motions During Catalysis by Dihydrofolate Reductases. *Philos. Trans. R. Soc., B 361*, 1317−1321.
(31) Wang, X., Chan, T. F. A. I., Lam, V. M. S., and Engel, P. C. (2008) What is the role of the second "structural" $NADP^+$ binding site in human glucose 6-phosphate dehydrogenase? *Protein Sci. 17*, 1403−1411.
(32) Zakrzewski, S. F., and Sansone, A. M. (1971) A new synthesis of tetrahydrofolic acid. *Methods Enzymol. 18*, 728−731.
(33) Delaglio, F., Grzesiek, S., Vuister, G. W., Zhu, G., Pfeifer, J., and Bax, A. (1995) Nmrpipe: A Multidimensional Spectral Processing System Based on Unix Pipes. *J. Biomol. NMR 6*, 277−293.
(34) Vranken, W. F., Boucher, W., Stevens, T. J., Fogh, R. H., Pajon, A., Llinas, M., Ulrich, E. L., Markley, J. L., Ionides, J., and Laue, E. D. (2005) The CCPN data model for NMR spectroscopy: Development of a software pipeline. *Proteins: Struct., Funct., Genet. 59*, 687−696.
(35) Loveridge, E. J., Matthews, S. M., Williams, C., Whittaker, S. B. M., Günther, U. L., Evans, R. M., Dawson, W. M., Crump, M. P., and Allemann, R. K. (2013) Aliphatic ^1H, ^{13}C and ^{15}N chemical shift assignments of Dihydrofolate reductase from the psychropiezophile *Moritella profunda* in complex with $NADP^+$ and folate. *Biomol. NMR Assignments 7*, 61−64.
(36) Loveridge, E. J., Tey, L. H., Behiry, E. M., Dawson, W. M., Evans, R. M., Whittaker, S. B. M., Günther, U. L., Williams, C., Crump, M. P., and Allemann, R. K. (2011) The Role of Large-Scale Motions in Catalysis by Dihydrofolate Reductase. *J. Am. Chem. Soc. 133*, 20561−20570.
(37) Osborne, M. J., Venkitakrishnan, R. P., Dyson, H. J., and Wright, P. E. (2003) Diagnostic chemical shift markers for loop conformation and substrate and cofactor binding in Dihydrofolate reductase complexes. *Protein Sci. 12*, 2230−2238.
(38) Williamson, M. P. (2013) Using chemical shift perturbation to characterise ligand binding. *Prog. Nucl. Magn. Reson. Spectrosc. 73*, 1−16.
(39) Ohmae, E., Sasaki, Y., and Gekko, K. (2001) Effects of Five-Tryptophan Mutations on Structure, Stability and function of Escherichia coli Dihydrofolate Reductase. *J. Biochem. 130*, 439−447.
(40) Ben-Bassat, A., Bauer, K., Chang, S. Y., Myambo, K., Boosman, A., and Chang, S. (1987) Processing of the initiation methionine from proteins: properties of the Escherichia coli methionine aminopeptidase and its gene structure. *J. Bacteriol. 169*, 751−757.
(41) Schnell, J. R., Dyson, H. J., and Wright, P. E. (2004) Structure, dynamics, and catalytic function of dihydrofolate reductase. *Annu. Rev. Biophys. Biomol. Struct. 33*, 119−140.
(42) Venkitakrishnan, R. P., Zaborowski, E., McElheny, D., Benkovic, S. J., Dyson, H. J., and Wright, P. E. (2004) Conformational changes in the active site loops of dihydrofolate reductase during the catalytic cycle. *Biochemistry 43*, 16046−16055.
(43) Hajduk, P. J., Augeri, D. J., Mack, J., Mendoza, R., Yang, J., Betz, S. F., and Fesik, S. W. (2000) NMR-based screening of proteins containing ^{13}C-labelled methyl groups. *J. Am. Chem. Soc. 122*, 7898−7904.
(44) Behiry, E. M., Evans, R. M., Guo, J., Loveridge, E. J., and Allemann, R. K. (2014) Loop Interactions During Catalysis by Dihydrofolate Reductase from *M. profunda*. *Biochemistry 53*, 4769−4774.
(45) Weikl, T. R., and Boehr, D. D. (2012) Conformational selection and induced changes along the catalytic cycle of *Escherichia coli* dihydrofolate reductase. *Proteins: Struct., Funct., Genet. 80*, 2369−2383.
(46) Boehr, D. D., Dyson, H. J., and Wright, P. E. (2008) Conformational Relaxation following Hydride Transfer Plays a Limiting Role in Dihydrofolate reductase Catalysis. *Biochemistry 47*, 9227−9233.
(47) Mauldin, R. V., and Lee, A. L. (2010) NMR study of the role of M42 in the solution dynamics of E.COLI dihydrofolate reductase. *Biochemistry 49*, 1606−1615.

DOI: 10.1021/acs.biochem.7b00045
Biochemistry 2017, 56, 2126−2133